

## Article

# Research of a Novel Non-Axisymmetric Side-Compressed Variable Polarity Plasma Arc and Its Pressure Distribution Characteristics

Hongxing Zhao, Chunli Yang and Chenglei Fan \*

State Key Laboratory of Advanced Welding and Joining, Harbin Institute of Technology, Harbin 150001, China; hxingzhao@163.com (H.Z.); yangcl9@hit.edu.cn (C.Y.)

\* Correspondence: fclwh@hit.edu.cn

**Abstract:** In the keyhole variable polarity plasma arc welding (VPPAW) process at horizontal position, the metal driven by gravity gathered on one side of the molten pool, and the weld formation is difficult, especially for thick workpiece welding. A specially designed experiment to analyze the influence of gravity on weld formation and a novel nozzle structure with side holes was proposed to generate a novel non-axisymmetric side-compressed plasma arc and redistribute arc pressure. The arc shape and pressure distribution were studied, and the ratio of difference for arc pressure in different directions  $R_p$  was introduced to evaluate the effects of non-axisymmetric side compression for the plasma arc. The results indicate that the non-axisymmetric distributed side holes reshape the plasma arc both in the EN and EP phases. The pressure of the non-axisymmetric side-compressed plasma arc decreases relatively strongly in one direction (direction b) and relatively weakly in the other direction (direction a).  $R_p$  is significant at 1 mm to 5 mm from the arc center, with a relatively large  $R_p$  within this range. The compression effect is enhanced with an increase in welding current or plasma gas flow rate, and  $R_p$  increases from 24% to 49% as the plasma gas flow rate increases from 2 L/min to 4.5 L/min. Specially designed validation experiments confirm that the new plasma arc significantly affects the weld formation in keyhole VPPAW process. An aluminum alloy workpiece with 8 mm thickness and no groove preparation was welded by the novel plasma arc in a horizontal welding position, and the weld is well formed.

**Keywords:** keyhole variable polarity plasma arc welding; non-axisymmetric side-compressed plasma arc; arc pressure; horizontal position; PAW; novel nozzle



**Citation:** Zhao, H.; Yang, C.; Fan, C. Research of a Novel Non-Axisymmetric Side-Compressed Variable Polarity Plasma Arc and Its Pressure Distribution Characteristics. *Metals* **2024**, *14*, 231. <https://doi.org/10.3390/met14020231>

Academic Editor: Masahiro Fukumoto

Received: 2 January 2024

Revised: 7 February 2024

Accepted: 12 February 2024

Published: 14 February 2024



**Copyright:** © 2024 by the authors. Licensee MDPI, Basel, Switzerland. This article is an open access article distributed under the terms and conditions of the Creative Commons Attribution (CC BY) license (<https://creativecommons.org/licenses/by/4.0/>).

## 1. Introduction

In the manufacturing process of large equipment, limited by size and weight, there is a demand for welding in the horizontal position. Arc welding is a widely utilized welding process to join various structural alloys, including steel and aluminum alloys. However, arc welding techniques such as GMAW and GTAW require multiple passes to join thick plates [1,2]. Among arc welding processes, plasma arc has a high energy density to weld thick workpieces. Variable polarity plasma arc welding (VPPAW) is a particular type of plasma arc welding that cleans the oxide film on the surface of the weld during the electrode positive (EP) phase. In a horizontal welding position, the liquid metal tends to gather towards the lower side of the molten pool due to the influence of gravity [3], in the process of keyhole plasma arc welding. As a result, it is difficult to achieve a good weld formation of aluminum alloy with a thickness of 8 mm and above [4], using the axisymmetric variable polarity plasma arc in a horizontal position.

In the fusion welding process, the heat source usually has two effects on the molten pool: heat and force [5]. In general, heat is first in the spotlight and discussed, as it is directly related to metal melting. However, in the keyhole plasma arc welding process, the force exerted by the arc is a critical factor in maintaining the keyhole shape and deciding

the weld formation. In the keyhole welding process, controlling the keyhole molten pool is the key to weld formation [6–13].

In a horizontal welding position, the porosity of weld may be increased and undermine mechanical properties of the weld, because outflow of gas in the molten pool is hindered by the solid upper side base metal. Yan et al. investigated the microstructure, porosity, and mechanical properties of horizontal position VPPAW welded joints of 5A06 aluminum alloy with 5 mm thickness [3,14,15]. In a horizontal position, the asymmetric metal flow induced by gravity led to uneven grain size and low-angle grain boundary distribution in the welded joint. The microhardness distribution in the joint was non-uniform, and the tensile fracture occurred on the upper side of the welded joint.

It is an effective method to change arc characteristics by additional gas flow [16,17]. Li et al. proposed gas focused plasma arc by utilizing an additional gas to radially compress the plasma arc, resulting in an axisymmetrical plasma arc [18,19]. As the arc voltage increased, the energy was enhanced, but there was no obvious change in arc pressure.

Compared with other arcs, plasma arc pressure is larger, which is a critical factor in determining the weld formation. Wang's research [20] shows that the maximum arc pressure of the plasma-TIG coupled arc depends mainly on the welding current and plasma gas flow rate of the plasma arc. Chen studied the characteristics of pulsed plasma arc pressure [21], the arc pressure changed cyclically with the pulsed plasma arc on and off. Xu studied the secondary compression effect of keyhole on plasma arc pressure through numerical simulation [22]. The simulation results show that arc pressure increases significantly at the minimum diameter of the keyhole.

The shape and size of the orifice on the nozzle are critical factors for the keyhole size and arc pressure in the PAW process [23,24]. The smaller orifice diameter increases the arc compression degree, resulting in an increase in the arc pressure, while the max carry current of the nozzle is reduced.

Zhang introduced soft VPPAW with two side holes on the nozzle, aiming to reduce plasma arc pressure [4,25]. Simultaneously, an 8 mm-thick aluminum alloy plate with a Y-shaped groove was welded by keyhole soft VPPAW in a horizontal position, and the weld was well formed. For soft VPPAW in a horizontal position, a groove is needed to weld an 8 mm-thick plate, and it is challenging to weld a thicker plate. The arc pressure and current density distributions of soft plasma arc are measured and treated as axisymmetric in these research papers.

Typically, since the torch and gas flow are axisymmetric, the arc is also idealized as an axisymmetrical structure. However, in some welding positions, such as horizontal position, to maintain the force balance on the molten pool, the symmetrical arc is not necessarily the optimal structure. The non-axisymmetric plasma arc and its arc pressure distribution are rarely studied.

This paper focuses on the arc characters of the new designed plasma arc, which is redistributed by non-axisymmetric side holes on the nozzle. The unique heat source requirements for horizontal position welding were studied, providing a fundamental basis for the new nozzle design. The arc morphology was captured by high-speed camera. The arc pressure distribution of the plasma arc was measured using a pressure measuring system. The influence of non-axisymmetric side compression on plasma arc pressure distribution and compression degree is evaluated. A special experiment was designed to verify the influence of the new heat source on the weld formation in the VPPAW process. Aluminum alloy of 8 mm thickness was welded by the new non-axisymmetric side-compressed plasma arc in the horizontal position, to verify the adaptability of the new heat source to horizontal position welding.

## 2. Experimental Procedures

### 2.1. Materials and Devices

The experiment setup is shown in Figure 1a. The system consists of power source, torch, motion platform, cooling water tank, wire feeder, gas supply, and controller. The

maximum welding current of the welding equipment is 300 A. The base material was AA2024 aluminum alloy with a size of  $300 \times 150 \times 8 \text{ mm}^3$ . The filler wire is ER2319, and its diameter is 1.6 mm. During the experiment, the electrode in the torch was W-2%ThO<sub>2</sub>, with a diameter of 4.8 mm. Argon was chosen as the shielding gas and plasma gas, and the flow rate of the shielding gas was 15 L/min. The welding current range was 80–245 A, and the plasma gas flow rate ranged from 2.0 to 4.5 L/min. In the VPPAW process, the time of EN and EP was 21 ms and 4 ms, respectively, in a single cycle.

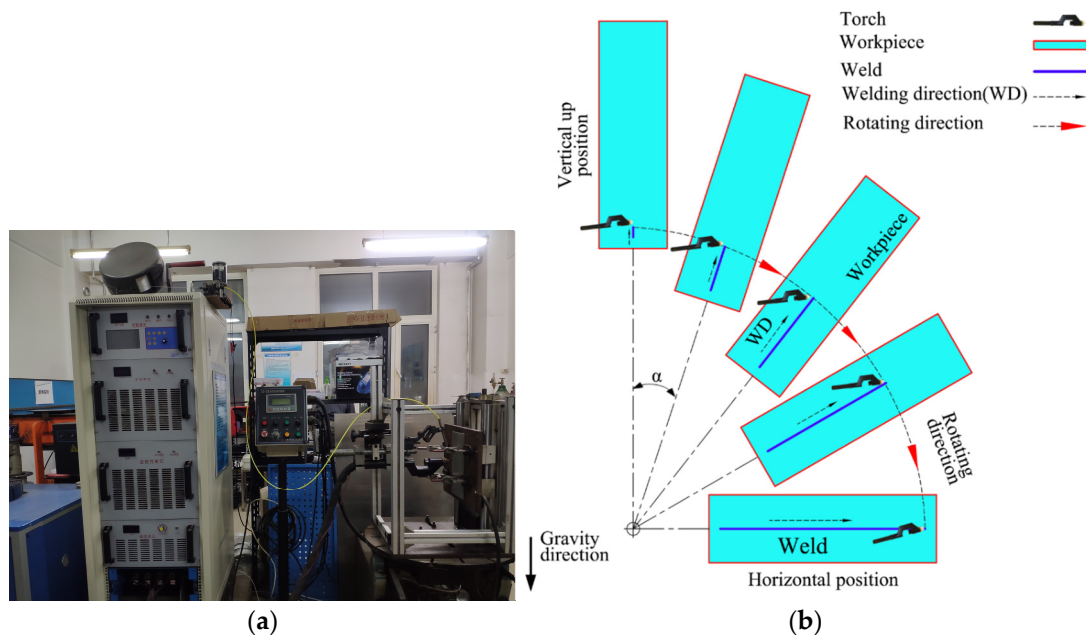


**Figure 1.** The equipment and diagram of the welding experiment: (a) experimental setup; (b) diagram of keyhole VPPAW process with continuously varying positions from vertical-up to horizontal positions.

The weld is most easily formed in the vertical-up welding position in keyhole plasma arc welding process. Compared with the vertical-up welding position, it is difficult to obtain good weld formation in horizontal welding position. A new process was proposed to gradually vary the welding position from vertical-up to the horizontal position on the same weld, to analyze the influence of the welding position on the weld formation, and to provide a basis for the new heat source. The welding motion platform consists of two parts: the linear motion platform and the rotational motion mechanism, which can carry out rotational motion while the workpiece moves in a straight line, as shown in Figure 1b.

Plasma arc topography was captured by a high-speed camera, the camera type is Phantom V311 (Vision Research, Wayne, NJ, USA). During the shooting process, to ensure the arc's consistency and avoid the plate melting due to the thermal effect of the arc, a water-cooled copper plate served as anode. When shooting plasma arcs, the high-speed camera frame rate is 1000 fps, and the exposure time is 4  $\mu\text{s}$ .

The arc pressure sensing and measuring device is shown in Figure 2. The system consists of a water-cooled copper plate with a small guiding hole, an insulated connecting pipe, a pressure sensor, a metering resistor, and a data acquisition subsystem. During the measurement process, the plasma enters the pressure sensor, passes through the small hole on the water-cooled copper plate and the insulated connecting pipe, converts the pressure signal into current signal [26], and is input by the metering resistor. By measuring the voltage on the metering resistor, the pressure at the small hole of the water-cooled copper plate is calculated. During the measurement process, the acquisition frequency of the data acquisition card is 20 kHz. During the experiment, the arc pressure distribution on the anode surface was measured by moving the measuring device to scan it line by line. During the scanning process, the platform moves at 1 mm/s.

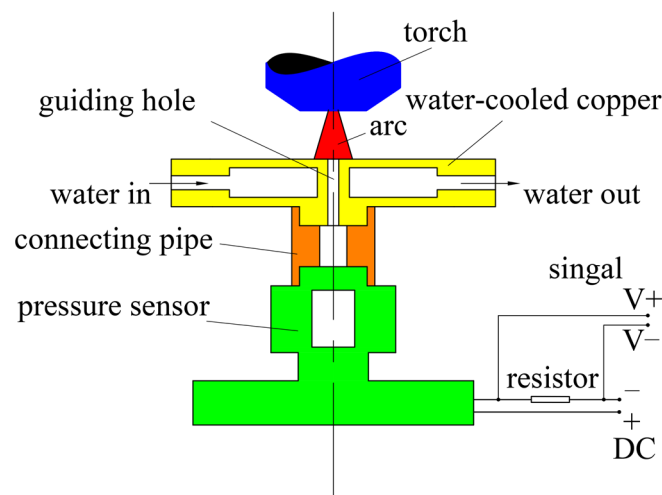


**Figure 2.** Arc pressure measuring device.

## 2.2. Weld Formation

To understand the unique requirements of heat source for keyhole VPPAW process in horizontal position, an experiment was designed to study the influence of gravity on keyhole welding process. By changing the relative direction of gravity action on the same straight weld, as shown in Figure 1b, the welding position is gradually changed from vertical-up to horizontal position in the VPPAW process.

During the experiment, the workpiece was driven by a linear motion platform, which was attached to a mechanism that can be rotated and driven by the rotational motion mechanism, as shown in Figure 1. In the initial state (rotation angle  $\alpha = 0^\circ$ ), the linear motion platform drives the workpiece to move downward, and the workpiece is in the vertical-up VPPA welding process. In the welding process, the rotational motion mechanism rotates the workpiece, torch, and the linear motion platform to change the angle between the welding direction and the gravity direction. As the rotational motion mechanism drives the whole linear moving platform to rotate, the welding position gradually changes from vertical-up ( $\alpha = 0^\circ$ ) to horizontal position ( $\alpha = 90^\circ$ ). Finally, the process of varying from vertical-up to horizontal welding position is shown on one single straight weld. By comparing the influence of the change in the angle between the gravity direction and the welding direction on the weld formation, it provides the experimental basis for proposing the heat source requirements of horizontal position welding.

In the welding process, the rotational speed was about  $1.4^\circ/\text{s}$  and the welding speed was  $150 \text{ mm}/\text{min}$ . The welding currents of EP and EN were  $245 \text{ A}$  and  $205 \text{ A}$ . The plasma gas and shielding gas flow rates were  $2.8 \text{ L}/\text{min}$  and  $15 \text{ L}/\text{min}$ , respectively.

The VPPAW weld that position changed from vertical-up to horizontal position is shown in Figure 3. At the beginning of the weld, the face and back of the weld are well-filled, and the width of the back of the weld is small. As the platform changes from vertical to horizontal welding position, under the action of gravity, the width of face of the weld does not change much. The metal in the molten pool gradually gathers to one side of the weld (lower side), while the side that deviates from the direction of gravity (upper side) has begun to undercut. The depth of the undercut increases with the rotation angle ( $\alpha$ ) increasing.

On the back of the weld, the width and height of the back of the weld increase significantly with the increase in the rotation angle  $\alpha$ . The width of the back of the weld increased from  $4.26 \text{ mm}$  at the starting position to  $8.92 \text{ mm}$  before cutting, an increase of almost  $109\%$ . Eventually, when the rotation angle  $\alpha$  reaches a certain degree, the molten pool becomes unstable, resulting in the weld beginning to be cut. After the weld starts to be cut, most of the liquid metal in the molten pool accumulates on the lower and back sides of the weld, with minimal metal remaining on the upper side.

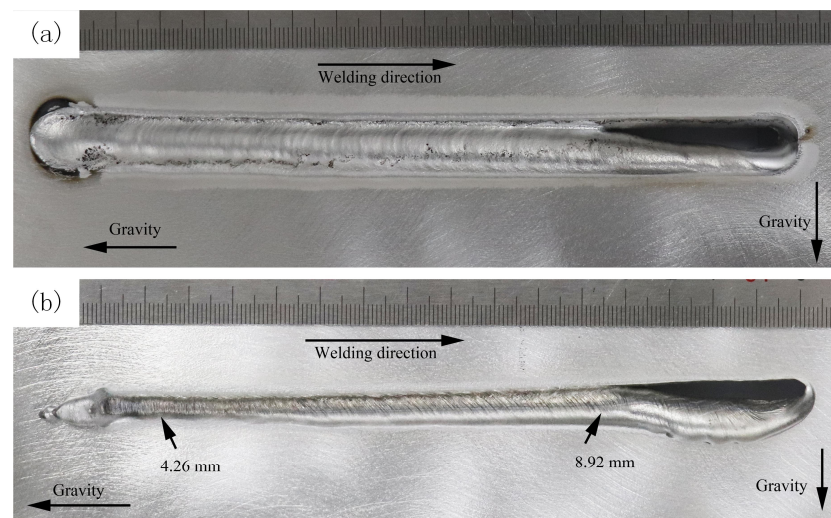


**Figure 3.** Morphology of weld welded by keyhole VPPAW with continuously varying position from vertical position to horizontal position (8 mm-thick aluminum alloy): (a) face of the weld; (b) back side.

### 2.3. New Nozzle

The weld morphology in Figure 3 indicates that as the welding position rotates closer to the horizontal position, metals gradually gather to the lower side and back side of the weld. Metal accumulation to the lower side of the weld is mainly caused by gravity. Meanwhile, the accumulation of metals towards the back side indicates that the driving force to promote molten pool metal flow to the back side of the weld is too strong, while the driving force to promote the backfilling of molten pool metal to the face of the weld is insufficient. This is also the main reason why keyhole VPPAW formation is difficult in horizontal position.

To achieve a balanced, stable keyhole VPPAW process in a horizontal position, it is necessary to increase the driving force as well as decrease the resistance of molten pool metal flow to the face and reduce the size of the molten pool to reduce the influence of gravity on the welding process. For keyhole VPPAW welding process, arc pressure is the resistance of metal reflow to the face, and surface tension is the driving force of metal reflow to the face on the rear side of the molten pool [27], which is discussed later. It is necessary to reduce the arc pressure of the heat source and the size of the molten pool in horizontal position welding.

Several methods can compress the arc, such as applying an additional energy field or adding a new gas path to focus the arc [16,17,19,28,29]. There are also methods that use side holes of the nozzle to compress the plasma arc, such as soft plasma arc [4]. These methods have certain advantages, but there are few studies about these methods in the PAW process in horizontal position. Based on the above weld formation study and the requirements of plasma arc for horizontal position welding, a new nozzle was designed.

A new type of nozzle with non-axisymmetric distributed side holes is designed to second compress the plasma arc in a specific direction by the plasma gas outflowing from side holes. In contrast, the arc characteristics in the other direction are less affected. The conventional nozzle and the new nozzle are shown in Figure 4. Since the flow from the side hole comes from the plasma gas, this method does not require an additional gas circuit.

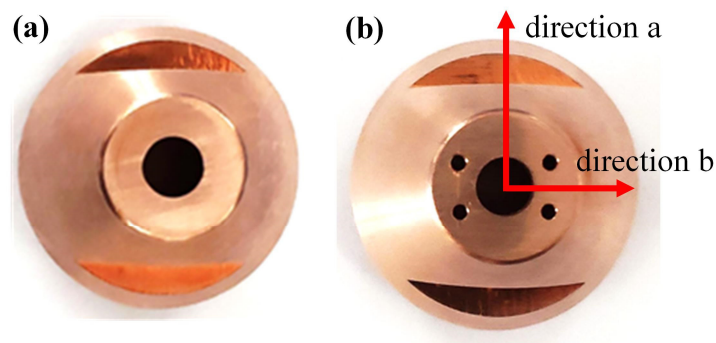


**Figure 4.** Conventional nozzle and newly designed nozzle to compress plasma arc: (a) conventional nozzle; (b) newly designed nozzle.

### 3. Results

#### 3.1. Morphology

In a non-axisymmetric side-compressed variable polarity plasma arc (NASSC-VPPA), the arc is compressed by the central orifice of the nozzle. After the plasma flows out of the nozzle through the central orifice, it will be compressed secondly by the gas flowing out from the nozzle through the side holes.

Under the secondary compression of the gas flow from the side holes of the nozzle, the plasma arc will show a unique non-axisymmetric characteristic. Directions a and b are defined as shown in Figure 4, with directions a and b perpendicular to each other. A high-speed camera was used to observe the shape of NASSC-VPPA in direction a and direction b. The welding current was 180 A at both the Electrode Negative (EN) and EP phases. The time of EN and EP were 21 ms and 4 ms, respectively.

Plane a is defined as the plane which consists of the direction a and the center line of the arc. Plane b is defined as the plane which consists of the direction b and the center line of the arc. As shown in Figure 5, in EN and EP phases, the plasma arc morphology is different in plane a and plane b. The maximum widths of arc were measured in planes a and b, in the VPPA process. During the EN phase, the arc widths in planes a and plane b were 9.4 mm and 8.5 mm, respectively. Meanwhile, in the EP phase, the arc widths in planes a and plane b were 9.4 mm and 8.1 mm, respectively.

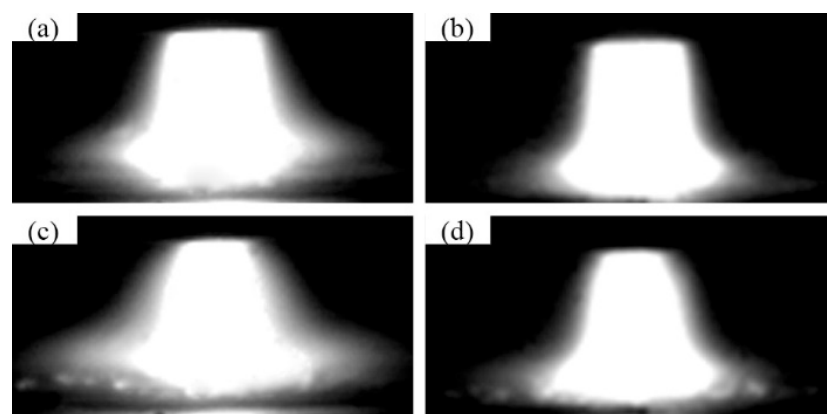


**Figure 5.** Morphology of variable polarity plasma arc in different planes: (a) plane a during the EN phase; (b) plane b during the EN phase; (c) plane a during the EP phase; (d) plane b during the EP phase.

The measurement results show that the arc width in plane a is broader than that in plane b in both EN and EP phases, indicating that the arc shape of variable polarity plasma arc is affected by non-axisymmetric distributed side holes, and the arc shape is compressed in direction b.

### 3.2. Arc Pressure

The arc pressure measurement system was employed for line-by-line scanning to measure the distribution of plasma arc pressure and the distribution of plasma arc pressure on the anode surface was obtained. Firstly, the anode arc pressure distribution of the plasma arc with a conventional nozzle was measured systematically. As shown in Figure 6, in directions a and b, the arc pressure of the plasma arc with conventional nozzle is almost the same in directions a and b.

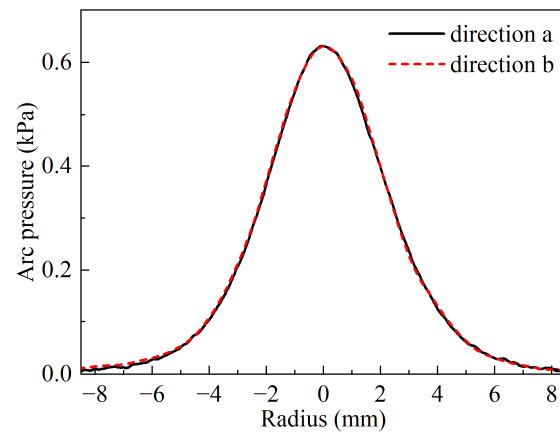


**Figure 6.** Arc pressure distribution of plasma arc with a conventional nozzle on anode surface in directions a and b.

The same equipment and method were used to measure the non-axisymmetric side-compressed plasma arc (NASSC-PA). The welding current (EN) was 100 A, and the plasma gas flow rate was 3.5 L/min. The distribution of arc pressure in directions a and b is shown in Figure 7. Compared with direction a, arc pressure decreases in direction b, and this decrease is more obvious within the range of 1 mm to 5 mm from the arc center.

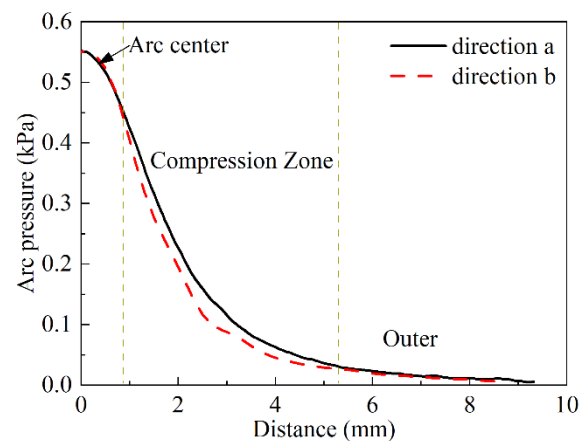


**Figure 7.** Arc pressure distribution of non-axisymmetric side-compressed plasma arc in directions a and b with welding current is 100 A.

The experimental results showed that the plasma arc pressure distribution can be changed effectively by using the nozzle with non-axisymmetric distributed side holes. The arc pressure distribution is different in directions a and b, and the arc pressure distribution is no longer axisymmetric.

When welding thicker workpieces by plasma arc, it is typically necessary to use a larger welding current and plasma gas flow rate to ensure that the arc has enough energy and pressure to form and maintain a keyhole molten pool. Therefore, it is necessary to verify the arc characteristics of the new nozzle structure under the conditions of large

current and plasma gas flow rate, to ensure the applicability of the new heat source in the thick-plate welding.

### 3.2.1. Different Welding Current

Arc pressure distribution of NASSC-PA under different current conditions is measured to analyze the influence of welding current on arc pressure distribution. The plasma gas and shielding gas flow rates are 3.5 L/min and 15 L/min, respectively, and the welding current (EN) ranges from 80 to 160 A.

The distribution of arc pressure in direction a and the maximum value of arc pressure under different current conditions are illustrated in Figure 8. The results show that the arc pressure increases with the increase in welding current, and the relationship between the maximum arc pressure and welding current is close to linear.

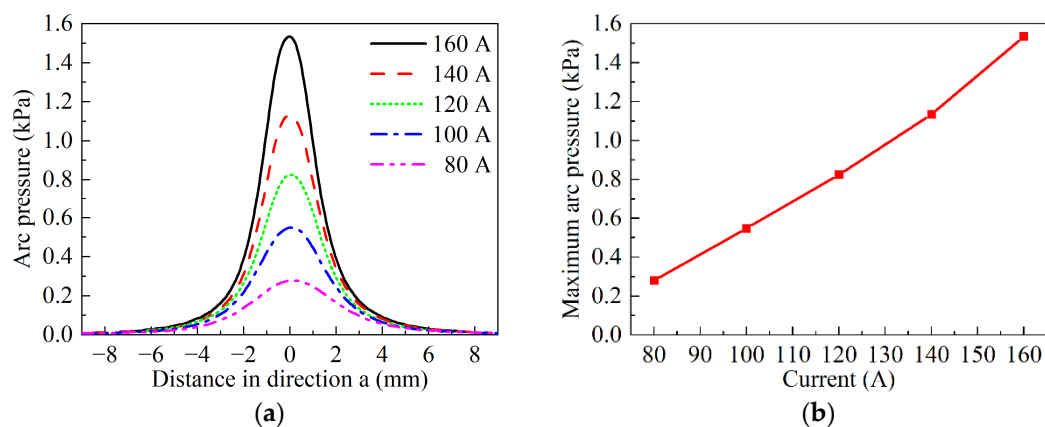


**Figure 8.** Arc pressure of NASSC-PA with different welding currents: (a) arc pressure distribution in direction a; (b) maximum arc pressure with different welding currents.

The welding current (EN) is 80 A and 140 A, and the distribution of arc pressure of NASSC-PA in directions a and b is depicted in Figure 9. The distribution of plasma arc pressure in directions a and b is different. Compared with the arc pressure distribution while the welding current is 80 A, the difference in arc pressure distribution in direction a and direction b is greater when the welding current is 140 A.

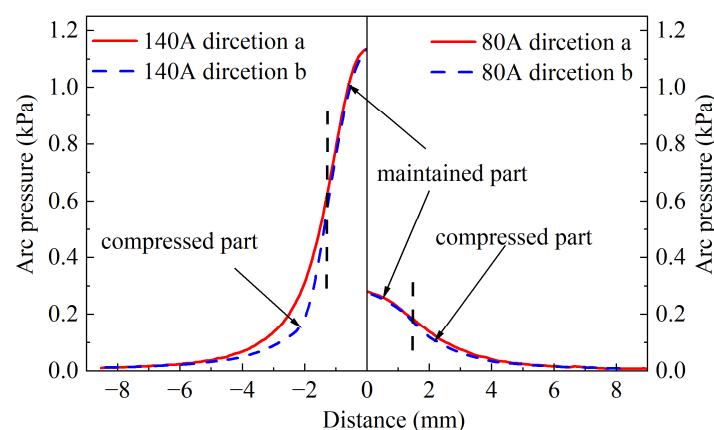


**Figure 9.** The arc pressure distribution of NASSC-PA with welding current is 140 A and 80 A in directions a and b.

### 3.2.2. Different Plasma Gas Flow Rate

In NASSC-PA, the side holes provide new outflow channels for the gas particles inside the nozzle. Some particles flow out from the nozzle through the center orifice, and the others flow out through the side holes. However, due to the high temperature of the gas

flowing out of the nozzle, it is difficult to measure the flow rate of the holes directly through the conventional measurement device. According to the conservation law of mass, the flow rate of plasma gas is the sum of the center orifice's flow rate and the side holes' flow rate. In general, when the plasma gas flow rate increases, the flow rate of side holes and center orifice also increases. Therefore, it is reasonable to evaluate the influence of side holes and center orifice flow rates on plasma arc pressure by plasma gas flow rate.

Measuring the arc pressure distribution of the NASSC-PA, as shown in Figure 10. The welding current is 120 A, and the plasma gas flow rate increases from 2 L/min to 4.5 L/min. It is evident that the arc pressure significantly increases with the plasma gas flow rate increasing. Within the measured plasma gas flow rate range, the maximum arc pressure exhibits an approximately linear relationship with the plasma gas flow rate.

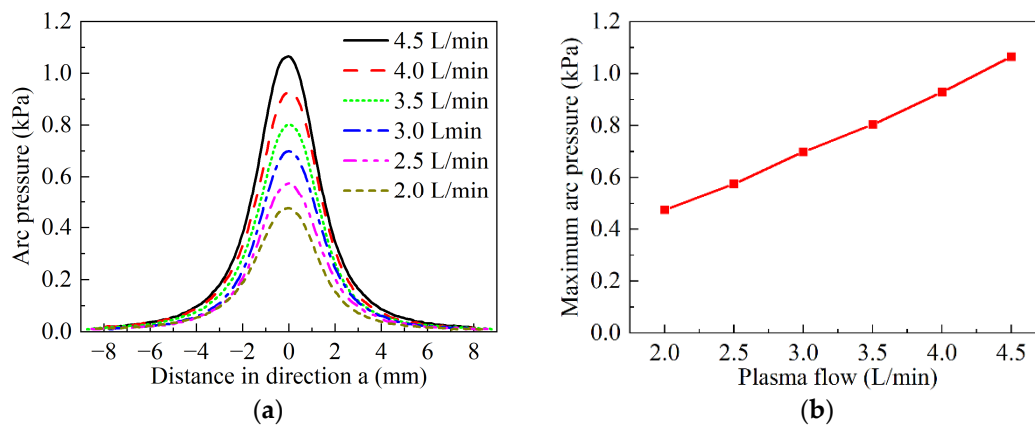


**Figure 10.** Arc pressure of NASSC-PA with different plasma gas flow rates: (a) arc pressure distribution in direction a; (b) maximum arc pressure with different plasma gas flow rates.

Figure 11 shows the NRSSC-PA pressure distribution with plasma gas flow rates are 2 L/min and 4.5 L/min. Compared with the arc pressure distribution with a plasma gas flow rate of 2 L/min, the plasma arc pressure decreases more in direction b when the plasma gas flow rate is 4.5 L/min.

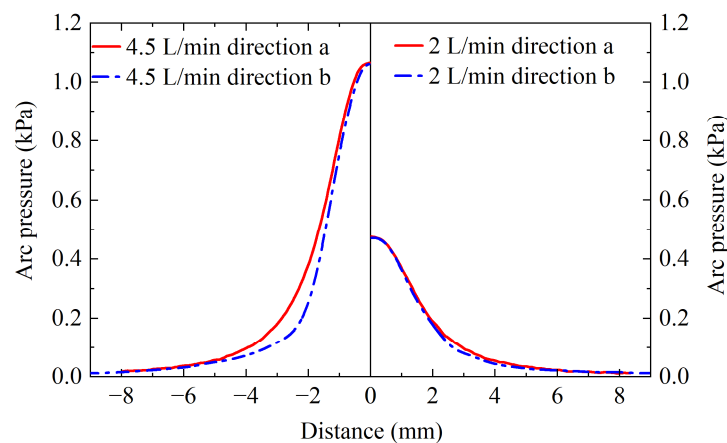


**Figure 11.** Arc pressure distribution of NASSC-PA with plasma gas flow rates of 4.5 L/min and 2 L/min in direction a and direction b.

#### 4. Discussion

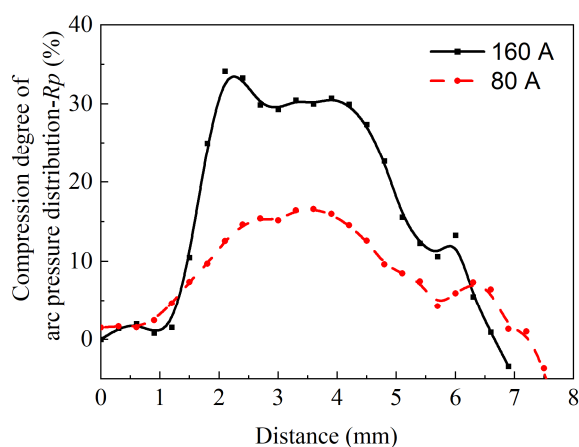
The plasma arc pressure distribution is different in different directions under the compression effect of non-axisymmetric distributed side holes. The compression degree of arc pressure distribution ( $R_p$ ) is defined in Equation (1), which describes the non-axisymmetric degree of arc pressure distribution to analyze the strength of non-axisymmetric compres-

sion.  $R_p$  is the ratio of the difference in arc pressure in directions a and b to the arc pressure in direction a, as Equation (1).

$$R_p = \frac{P_x(r) - P_y(r)}{P_x(r)} \times 100\% \tag{1}$$

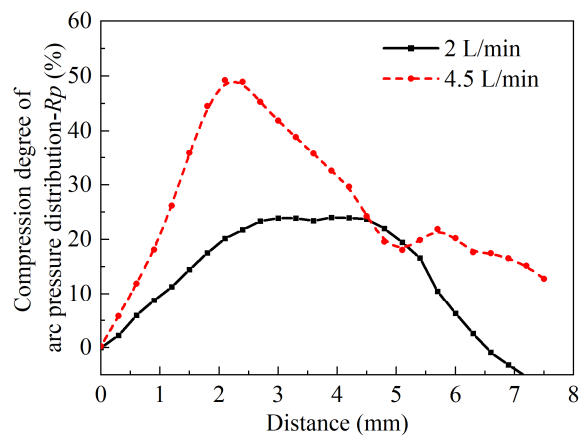
where  $P_x(r)$  and  $P_y(r)$  are the arc pressure at the same distance  $r$  from the arc center in direction a and direction b, respectively.

Figure 12 shows the compression degree coefficient  $R_p$  of plasma arc pressure under welding current of 80 A and 160 A. With an increase in distance from the arc center,  $R_p$  initially increases and then decreases. Near the center of the arc, the arc pressure in direction a and direction b is close, and  $R_p$  approaches 0%. In the range of 1 mm to 5 mm from the arc center, the asymmetry of the arc pressure distribution, characterized by  $R_p$ , is relatively large. However, beyond 5 mm from the arc center, the arc pressure is relatively small, and its impact on weld formation is minimal.



**Figure 12.** The compression degree of arc pressure distribution ( $R_p$ ) of NASSC-PA with different welding current.

Figure 13 shows  $R_p$  of arc pressure distribution at different positions, and the plasma gas flow rates are 2 L/min and 4.5 L/min. Similarly to Figure 12,  $R_p$  increases first and then decreases with the increase in distance from the arc center, and  $R_p$  is relatively large at the distance of 1 mm to 5 mm from the arc center. The maximum value of  $R_p$  increases from 24% to 49%, when the plasma gas flow rate increases from 2 L/min to 4.5 L/min.



**Figure 13.** The compression degree of arc pressure distribution ( $R_p$ ) of NASSC-PA with different plasma gas flow rates.

The above experimental results show that under the condition of high current and high plasma gas flow, the side holes with non-axisymmetric distribution still effectively impact the arc pressure distribution. The pressure of NASSC-PA distributes differently in different directions, and the pressure distribution decreases obviously in certain directions, such as direction b. The width of the weld may decrease when direction b is parallel to the direction of weld width since there is a smaller arc pressure impact.

The mechanism of side holes effect on plasma arc pressure distribution is analyzed. According to the ideal gas equation [24], as Equation (2), after entering the nozzle, plasma gas expands and its velocity increases, under the influence of high temperature of plasma arc. Some gas flows out the nozzle from the side hole to the arc space. In the arc space outside the nozzle, the high-temperature plasma particles collide with the relatively low-temperature gas particles flowing out from the side holes, and the energy and momentum transfer occurs. The transfer of energy and momentum reduces the temperature, velocity, and conductivity of the plasma in the nearby area, eventually leading to the compression of the arc and the reduction in the arc pressure in the nearby area.

$$PV = nRT \quad (2)$$

where  $P$  is the gas pressure,  $V$  is the gas volume,  $n$  is the number of moles,  $T$  is the gas temperature, and  $R$  is the universal gas constant,  $R = 8.31 \text{ J}/(\text{mol}\cdot\text{K})$ .

The plasma arc near the side hole is compressed and the arc pressure is reduced. Since the side holes are non-axisymmetrically distributed on the nozzle, the compression degree of the plasma arc is greater in a certain direction (such as direction b) and smaller in others. This ultimately results in a non-axisymmetric compressed plasma arc, and the arc pressure is non-axisymmetric distributed.

The above experimental results indicate that under the condition of high current and high orifice flow, the non-axisymmetric distributed side holes can still effectively compress the plasma arc, and the distribution of arc pressure is non-axisymmetric distributed. A special experiment is designed to validate the impact of the novel NASSC-VPPA on weld formation.

In the designed experiment, the angle between the compression direction (direction b) of the plasma arc and the welding direction is  $45^\circ$ , and the aluminum alloy with a thickness of 8 mm is welded by a non-axisymmetric side-compressed variable polarity plasma arc in a vertical-up position. In the vertical-up position, where gravity is parallel to the welding direction, the joint should be approximately left-right symmetrical when the workpiece is welded by the conventional variable polarity plasma arc in the keyhole model.

However, when using a non-axisymmetric side-compressed variable polarity plasma arc for keyhole welding, the angle between the compression direction (direction b) and the welding direction should be considered. As shown in Figure 14, the angle between the compression direction (direction b) of NASSC-VPPA and the welding direction is  $45^\circ$ , and the joint welded by the NASSC-VPPA consistently exhibits severe undercut on the left side while the right side forms well. The results indicate that non-axisymmetric side compression has a significant effect on the flow of the molten pool and weld formation in the keyhole VPPAW process.

The force acting on metal in a keyhole molten pool is analyzed, as shown in Figure 15. Molten pool metal is mainly affected by arc pressure ( $P$ ), surface tension ( $F_s$ ), electromagnetic force ( $F_m$ ), gravity ( $G$ ), buoyancy, and the supporting force ( $F_b$ ) of solid metal. Arc pressure and electromagnetic force depend on arc characteristics. The supporting force of solid metal on molten pool metal is reaction force, and its size and direction depend on the action of other forces.

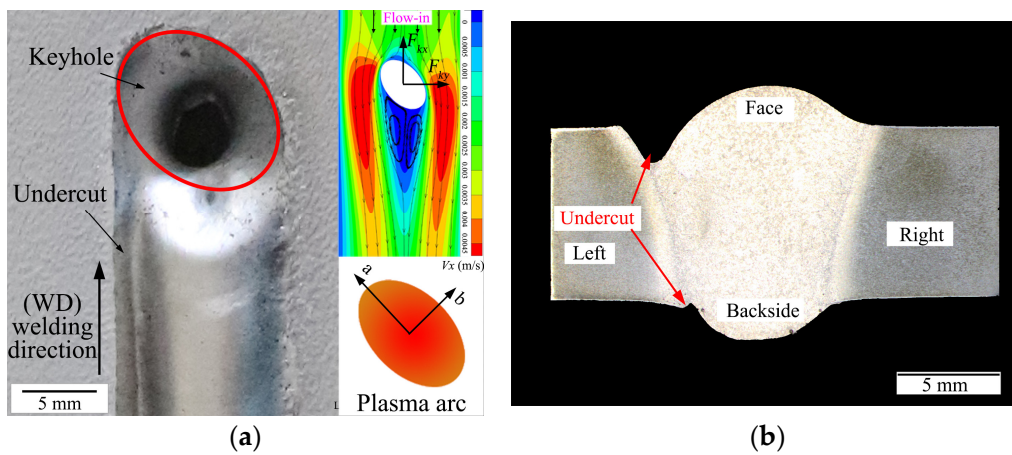


**Figure 14.** Weld formation of the specially designed experiment to validate the effect of non-axisymmetric side compression: (a) face of the weld, the angle between direction b and welding direction is 45 degrees; (b) cross-section of the weld.

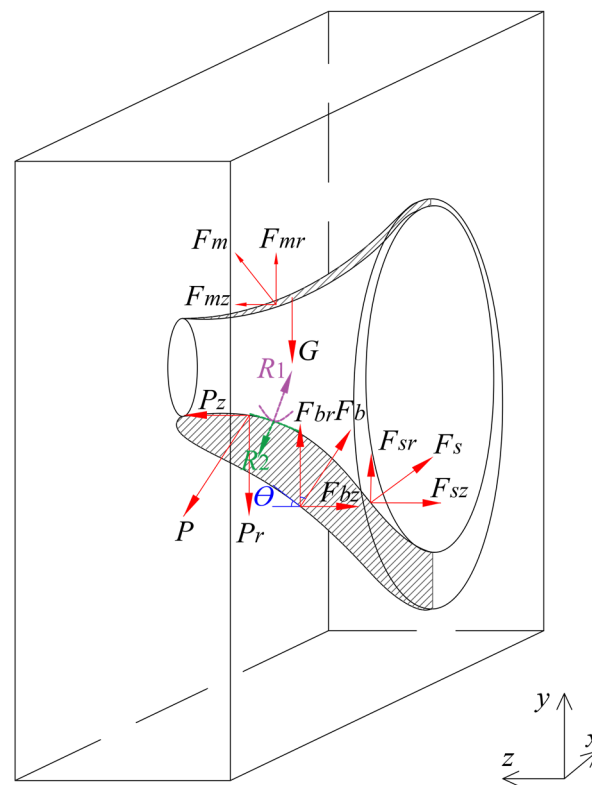


**Figure 15.** Force diagram of keyhole molten pool.

In the direction of workpiece thickness, the molten pool is mainly affected by arc pressure, surface tension, and the supporting force of solid metal. The object of the designed nozzle is to change the arc pressure distribution and the surface tension of the molten pool.

Additional pressure created by surface tension can be described by Young–Laplace’s equation, as Equation (3).  $\gamma$  is the surface tension coefficient, which is related to material and temperature.  $R_1$  and  $R_2$  are the curvature of the keyhole molten pool and related to the shape of the molten pool. Therefore, the impact of surface tension depends on the metal material of the molten pool, the temperature, and the shape of the keyhole molten pool. When the material and temperature of the molten pool remain unchanged, the surface tension of the molten pool increases with the decrease in molten pool curvature  $R_1$  and  $R_2$ . In keyhole VPPAW process, the size of the face of keyhole is larger than the size of the back

side, the surface tension is the driving force of metal reflow to the face in the rear side of the keyhole molten pool [27,30,31].

$$\Delta P = \gamma \left( \frac{1}{R_1} + \frac{1}{R_2} \right) \quad (3)$$

where  $\Delta P$  is the additional pressure created surface tension,  $\gamma$  is the surface tension coefficient, and  $R_1$  and  $R_2$  are the principal radii of curvature.

In the keyhole VPPAW process, the impact of surface tension can be enhanced by reducing the width of the molten pool, which will be beneficial to the reflow of the molten pool metal to the face [30,31].

The arc pressure, directed from the welding torch to the back side of the workpiece, is the resistance of molten pool metal reflowing to the face of the weld. Compared with other welding methods, the arc pressure of the plasma arc is larger due to the compression of the nozzle, which significantly affects the keyhole shape and weld formation.

Both reducing the arc pressure and decreasing the width of the molten pool to enhance the surface tension are conducive to the backfilling process of the molten pool metal, and it will promote the force balance of the VPPAW molten pool in a horizontal position.

The experimental result indicates that, on the one hand, the novel-designed nozzles with non-axisymmetric distributed side holes can significantly reduce the arc pressure in a certain direction, which reduces the driving force of molten pool metal flowing to the back of the weld. On the other hand, when the compression direction is parallel to the width of the weld, the width of the weld can be reduced, the additional pressure of the surface tension increases, and the impact of the surface tension is enhanced, resulting in the driving force of the molten pool metal flowing to the face of the weld being increased. In summary, non-axisymmetric side compression of variable polarity plasma arc is beneficial to the stability of VPPAW molten pool and weld formation in a horizontal position.

An aluminum alloy workpiece with a thickness of 8 mm was bead-on-plate welded by the novel non-axisymmetric side-compressed variable polarity plasma arc in a horizontal position to verify the new heat source. In the welding process, the welding currents were 205 A and 245 A in EN and EP phases, the plasma gas and shielding gas flow rate were 4.5 L/min and 15 L/min, the welding speed was 150 mm/min with no groove prepared. The weld was well formed, as shown in Figure 16, which means that the new heat source is suitable for keyhole VPPAW of medium-thick plate aluminum alloy in a horizontal position, which is difficult for conventional K-VPPAW.

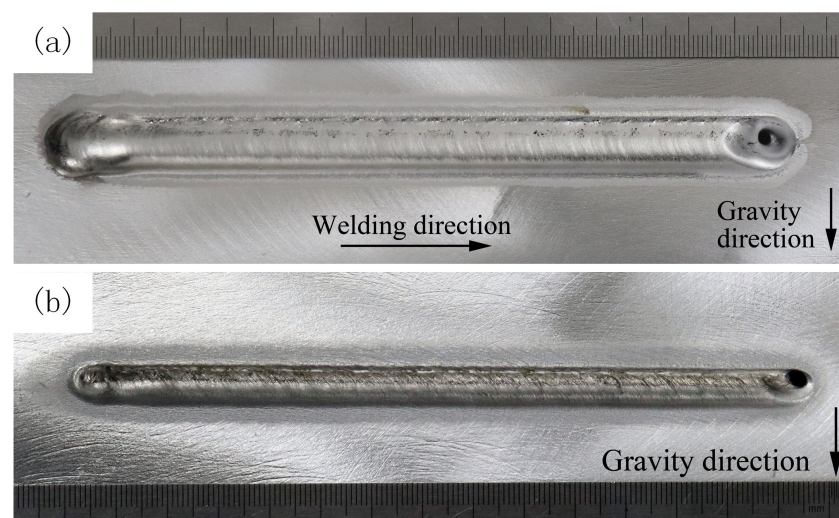


**Figure 16.** Weld formation of aluminum alloy by NASSC-VPPAW in a horizontal position while the thickness is 8 mm: (a) face of the weld (b) backside.

## 5. Conclusions

This paper designed a special experiment of the keyhole VPPAW welding process, in which the welding position was gradually changed from vertical to horizontal welding on one single straight weld for 8 mm-thick aluminum alloy. By analyzing the formation of this special weld, the requirements of heat source characteristics for horizontal position welding were clarified, and a new nozzle was designed to generate a novel non-axisymmetric side-compressed plasma arc. The plasma arc shape and arc pressure distribution generated by this new nozzle were analyzed, and the following conclusions can be drawn:

- (1) Smaller arc pressure and narrower molten pool width are needed for the keyhole VPPAW process in a horizontal position. A nozzle with non-axisymmetric distributed side holes was proposed to reshape the arc. The width of the plasma arc is smaller and compressed in direction b, both in the EP and EN phases.
- (2) The arc pressure of NASSC-PA is redistributed by the new nozzle. Compared with the arc pressure in direction a, the arc pressure is reduced in direction b, and the reduction is greater at 1 mm to 5 mm from the arc center.
- (3)  $R_p$  was defined to evaluate the compression degree of arc pressure. When welding current or plasma gas flow rate increased, the compression coefficient of arc pressure was still large. The maximum value  $R_p$  increases from 24% to 49% with the plasma gas flow rate increasing from 2 L/min to 4.5 L/min.
- (4) An aluminum alloy plate of 8 mm thickness with no groove preparation was welded by the new non-axisymmetric side-compressed variable polarity plasma in a horizontal position, with the compression direction (direction b) perpendicular to the welding direction, and a good weld formation was obtained, which breaks through the original plate thickness limit.

This new type of nozzle does not simply involve the addition of the side holes but also puts forward a new idea to change the arc characteristics. That is, it no longer merely increases or reduces the heat and force of the arc, but changes the heat and force characteristics of the arc in a specific direction, while a small change occurs in the other direction. The new nozzles redistribute the arc pressure of the plasma arc; meanwhile, the nozzles also have a significant effect on the arc energy distribution, which will be analyzed and discussed in another paper.

**Author Contributions:** Conceptualization, C.Y. and C.F.; methodology, H.Z. and C.Y.; validation, H.Z.; investigation, H.Z.; writing—original draft preparation, H.Z.; writing—review and editing, C.F.; supervision, C.Y. and C.F. All authors have read and agreed to the published version of the manuscript.

**Funding:** This research was supported by National Natural Science Foundation of China (No. 51475105).

**Data Availability Statement:** The data presented in this study are available on request from the corresponding author.

**Conflicts of Interest:** The authors declare no conflicts of interest.

## References

1. Serindağ, H.T.; Çam, G. Multi-Pass Butt Welding of Thick AISI 316L Plates by Gas Tungsten Arc Welding: Microstructural and Mechanical Characterization. *Int. J. Press. Vessel. Pip.* **2022**, *200*, 104842. [[CrossRef](#)]
2. Serindağ, H.T.; Çam, G. Characterizations of Microstructure and Properties of Dissimilar AISI 316L/9Ni Low-Alloy Cryogenic Steel Joints Fabricated by Gas Tungsten Arc Welding. *J. Mater. Eng. Perform* **2023**, *32*, 7039–7049. [[CrossRef](#)]
3. Yan, Z.; Chen, S.; Jiang, F.; Zhang, W.; Huang, N.; Chen, R. Control of Gravity Effects on Weld Porosity Distribution during Variable Polarity Plasma Arc Welding of Aluminum Alloys. *J. Mater. Process. Technol.* **2020**, *282*, 116693. [[CrossRef](#)]
4. Zhang, Q.L.; Fan, C.L.; Lin, S.B.; Yang, C.L. Novel Soft Variable Polarity Plasma Arc and Its Influence on Keyhole in Horizontal Welding of Aluminium Alloys. *Sci. Technol. Weld. Join.* **2014**, *19*, 493–499. [[CrossRef](#)]
5. Wu, C.S.; Wang, L.; Ren, W.J.; Zhang, X.Y. Plasma Arc Welding: Process, Sensing, Control and Modeling. *J. Manuf. Process* **2014**, *16*, 74–85. [[CrossRef](#)]
6. Li, Y.; Yun, Z.; Zhou, X.; Wu, C. Fundamental Understanding of Open Keyhole Effect in Plasma Arc Welding. *Phys. Fluids* **2023**, *35*, 043316. [[CrossRef](#)]

7. Miao, X.; Zhang, H.; Ge, F.; He, Z.; Gao, J.; Su, Z. Research on Arc Morphology and Keyhole Behavior of Molten Pool in Magnetically Controlled Plasma-GMAW Welding. *Metals* **2023**, *13*, 148. [[CrossRef](#)]
8. Li, Y.; Su, C.; Zhou, X.; Wu, C. A More Precise Unified Model to Describe Comprehensive Multiphysics and Multiphase Phenomena in Plasma Arc Welding. *J. Manuf. Process* **2020**, *59*, 668–678. [[CrossRef](#)]
9. Liu, J.; Jiang, F.; Xu, B.; Zhang, G.; Chen, S. Physical Mechanism of Material Flow and Temperature Distribution in Keyhole Plasma Arc Welding at Initial Unstable Stage. *Phys. Fluids* **2023**, *35*, 033115. [[CrossRef](#)]
10. Liu, J.; Jiang, F.; Chen, S.; Wang, K.; Zhang, G.; Xu, B.; Cheng, W.; Ma, X. Cross-Scale Process Quality Control of Variable Polarity Plasma Arc Welding Based on Predefined Temperature Field. *J. Mater. Res. Technol.* **2023**, *26*, 5347–5359. [[CrossRef](#)]
11. Xu, B.; Chen, S.; Tashiro, S.; Jiang, F.; Tanaka, M. Physical Mechanism of Material Flow in Variable Polarity Plasma Arc Keyhole Welding Revealed by in Situ X-Ray Imaging. *Phys. Fluids* **2021**, *33*, 017121. [[CrossRef](#)]
12. Wang, W.; Yamane, S.; Wang, Q.; Shan, L.; Sun, J.S.; Wei, Z.; Hu, K.; Lu, J.; Hirano, T.; Hosoya, K.; et al. Visual Sensing and Controlling of the Keyhole in Robotic Plasma Arc Welding. *Int. J. Adv. Manuf. Technol.* **2022**, *121*, 1401–1414. [[CrossRef](#)]
13. Lang, R.; Han, Y.; Bao, X.; Fan, J. Stability Mechanism of the Molten Pool in Variable Polarity Plasma Arc Welding of Medium Thickness Aluminum Alloy. *J. Mater. Process. Technol.* **2023**, *321*, 118127. [[CrossRef](#)]
14. Yan, Z.; Chen, S.; Jiang, F.; Zheng, X.; Tian, O.; Cheng, W.; Ma, X. Effect of Asymmetric Material Flow on the Microstructure and Mechanical Properties of 5A06 Al-Alloy Welded Joint by VPPA Welding. *Metals* **2021**, *11*, 120. [[CrossRef](#)]
15. Yan, Z.; Chen, S.; Jiang, F.; Zhang, W.; Huang, N. Study and Optimization against the Gravity Effect on Mechanical Property of VPPA Horizontal Welding of Aluminum Alloys. *J. Manuf. Process.* **2019**, *46*, 109–117. [[CrossRef](#)]
16. Zong, R.; Chen, J.; Wu, C. A Comparison of Double Shielded GMAW-P with Conventional GMAW-P in the Arc, Droplet and Bead Formation. *J. Mater. Process. Technol.* **2020**, *285*, 116781. [[CrossRef](#)]
17. Huu Manh, N.; Van Anh, N.; Van Tuan, N.; Xu, B.; Akihisa, M. Research and Development of a Novel TIG Welding Torch for Joining Thin Sheets. *Appl. Sci.* **2019**, *9*, 5260. [[CrossRef](#)]
18. Qing Li, T.; Yang, X.M.; Chen, L.; Zhang, Y.; Cheng Lei, Y.; Chun Yan, J. Arc Behaviour and Weld Formation in Gas Focusing Plasma Arc Welding. *Sci. Technol. Weld. Join.* **2020**, *25*, 329–335. [[CrossRef](#)]
19. Li, T.Q.; Chen, L.; Zhang, Y.; Yang, X.M.; Lei, Y.C. Metal Flow of Weld Pool and Keyhole Evolution in Gas Focusing Plasma Arc Welding. *Int. J. Heat Mass Transf.* **2020**, *150*, 119296. [[CrossRef](#)]
20. Wang, B.; Zhu, X.M.; Zhang, H.C.; Zhang, H.T.; Feng, J.C. Characteristics of Welding and Arc Pressure in the Plasma-TIG Coupled Arc Welding Process. *Metals* **2018**, *8*, 512. [[CrossRef](#)]
21. Chen, S.; Yan, Z.; Jiang, F. Arc Discharge and Pressure Characteristics in Pulsed Plasma Gas of PAW. *Int. J. Adv. Manuf. Technol.* **2019**, *102*, 695–703. [[CrossRef](#)]
22. Xu, B.; Jiang, F.; Chen, S.; Tanaka, M.; Tashiro, S.; Van Anh, N. Numerical Analysis of Plasma Arc Physical Characteristics under Additional Constraint of Keyhole. *Chin. Phys. B* **2018**, *27*, 034701. [[CrossRef](#)]
23. Short, A.B.; McCartney, D.G.; Webb, P.; Preston, E. Influence of Nozzle Orifice Diameter in Keyhole Plasma Arc Welding. *Sci. Technol. Weld. Join.* **2011**, *16*, 446–452. [[CrossRef](#)]
24. Stewart, M.I. Chapter Two—Basic Principles. In *Surface Production Operations*, 3rd ed.; Stewart, M.I., Ed.; Gulf Professional Publishing: Boston, MA, USA, 2014; Volume 2, pp. 9–37, ISBN 978-0-12-382207-9.
25. Zhang, Q.L.; Yang, C.L.; Lin, S.B.; Fan, C.L. Soft Variable Polarity Plasma Arc Horizontal Welding Technology and Weld Asymmetry. *Sci. Technol. Weld. Join.* **2015**, *20*, 297–306. [[CrossRef](#)]
26. Zhao, H.; Wang, G.; Song, J.; Liu, X.; Zhou, Z.; Yang, C. Comparative Research of Helium and Argon Arc Characters. *J. Mech. Eng.* **2018**, *54*, 137–143. [[CrossRef](#)]
27. Wu, D.; Chen, H.; Huang, Y.; He, Y.; Hu, M.; Chen, S. Monitoring of Weld Joint Penetration during Variable Polarity Plasma Arc Welding Based on the Keyhole Characteristics and PSO-ANFIS. *J. Mater. Process. Technol.* **2017**, *239*, 113–124. [[CrossRef](#)]
28. Wang, L.; Chen, J.; Wu, C.S. Auxiliary Energy-Assisted Arc Welding Processes and Their Modelling, Sensing and Control. *Sci. Technol. Weld. Join.* **2021**, *26*, 389–411. [[CrossRef](#)]
29. Qiao, J.; Wu, C.S. Concurrent Influence of Ultrasonic Vibration and Controlled Pulse Current on Plasma Arc Behaviors. *Int. J. Adv. Manuf. Technol.* **2022**, *119*, 811–826. [[CrossRef](#)]
30. Jarvis, B.L. Keyhole Gas Tungsten Arc Welding: A New Process Variant. Ph.D. Thesis, Faculty of Engineering, University of Wollongong, Wollongong, NSW, Australia, 2001.
31. Zhang, Q.; Yang, C.; Lin, S.; Sun, S.; Li, Z.; Liu, Z.; Jiang, Y.; Liu, J.; Ma, J. Research on Novel Soft Variable Polarity Plasma Arc Welding Technology for Aluminum Alloys in Horizontal Position. *J. Mech. Eng.* **2015**, *51*, 75–81. [[CrossRef](#)]

**Disclaimer/Publisher’s Note:** The statements, opinions and data contained in all publications are solely those of the individual author(s) and contributor(s) and not of MDPI and/or the editor(s). MDPI and/or the editor(s) disclaim responsibility for any injury to people or property resulting from any ideas, methods, instructions or products referred to in the content.